Smart Structures and Systems, *Vol. 25, No. 6 (2020) 643-655*
DOI: https://doi.org/10.12989/sss.2020.25.6.643

Active vibration control of nonlinear stiffened FG cylindrical shell under periodic loads

Habib Ahmadi* and Kamran Foroutan [a]

Faculty of Mechanical Engineering, Shahrood University of Technology, Shahrood, Iran

(*Received February 7, 2019, Revised December 5, 2019, Accepted February 4, 2020*)

Abstract. Active control of nonlinear vibration of stiffened functionally graded (SFG) cylindrical shell is studied in this paper. The system is subjected to axial and transverse periodic loads in the presence of thermal uncertainty. The material composition is considered to be continuously graded in the thickness direction, also these properties depend on temperature. The relations of strain-displacement are derived based on the classical shell theory and the von Kármán equations. For modeling the stiffeners on the cylindrical shell surface, the smeared stiffener technique is used. The Galerkin method is used to discretize the partial differential equations of motion. Some comparisons are made to validate the SFG model. For suppression of the nonlinear vibration, the linear and nonlinear control strategies are applied. For control objectives, the piezoelectric actuator is attached to the external surface of the shell and the thin ring piezoelectric sensor is attached to the middle internal surface of shell. The effect of PID, feedback linearization and sliding mode control on the suppression of vibration for SFG cylindrical shell is presented.

Keywords: nonlinear vibration; stiffened cylindrical shells; active control; functionally graded materials

1. Introduction

The SFG cylindrical shells are impressively utilized in variety of engineering systems such as bridges, offshore, submarines, ships, aircraft, and satellite structures. Thus, research on the vibration analysis of these structures has been done by scientists from many years ago. In recent years vibration control has been considered by using piezoelectric materials.

In vibration control of isotropic cylindrical shell, many researches have been concentrated on the active control of shells vibration with the linear controller. Kwak *et al.* (2012) presented the active control of a submerged cylindrical shell vibration with piezoelectric actuators and sensors using the method of Rayleigh-Ritz. Also, Kwak *et al.* (2009) addressed the active vibration control of the cylindrical shell by means of piezoelectric actuators and sensors. Hasheminejad and Oveisi (2016) studied active control of vibration for a type of circular cylindrical panel with piezoelectric sensor and actuator layers. Ma *et al.* (2014) coupled a two stage vibration isolation to an elastic cylindrical shell for active acoustic control of the system. A feedforward controller for analysis of active control of semi-infinite cylinder using a circumferential array of control forces and error sensors was presented by Pan and Hansen (1997). Biglar *et al.* (2014) used piezoelectric transducers for configurationally optimization and the active control of a cylindrical shell vibration. They derived dynamic modeling of shell by means of the method of Rayleigh-Ritz. Loghmani *et al.* (2017) investigated a linear quadratic Gaussian controller for vibration suppression of the cylindrical shell with piezo-ceramic actuators and sensors. The vibration response of a cylindrical shell using the concurrent active and passive damping treatments was analyzed by Plattenburg *et al.* (2017). Correia *et al.* (2002) presented active control of axisymmetric shell vibration with piezoelectric ring actuators and sensors.

Some researchers have studied the nonlinear analysis and vibration control of non-isotropic cylindrical shells and plates. The nonlinear axisymmetric response of FG shallow spherical shells resting on elastic foundation subjected to the uniform external pressure and temperature was studied by Duc *et al*. (2014). Cong *et al*. (2018) presented the nonlinear thermo-mechanical buckling and post-buckling response of FG porous plates utilizing Reddy’s HSDT. Thom *et al*. (2017) investigated the behavior of bi-directional FG plates by FEM and a new third-order shear deformation plate theory. The control of composite shell vibration using the optimized actuator and sensor systems were analyzed by Kim *et al.* (2001). Duc *et al*. (2019) addressed the free vibration and nonlinear dynamic response of imperfect nanocomposite FG-CNTRC double curved shallow shells under thermal condition. Tan and Vu-Quoc (2005) presented the active control of composite shell vibration with the optimal solid shell element. The static response and free vibration behavior of FG carbon nanotube-reinforced composite rectangular plates resting on elastic foundation were studied by Duc *et al*. (2017a). Duc and Cong (2018) investigated the nonlinear dynamic response and vibration of sandwich composite plates with negative Poisson’s ratio in auxetic honeycombs. Using the theory of first-order shear deformation, Sheng and Wang

*Corresponding author, Ph.D.,
E-mail: habibahmadif@shahroodut.ac.ir
[a] Ph.D. Student

ISSN: 1738-1584 (Print), 1738-1991 (Online)

(2010) studied the control of vibration for FG laminated piezoelectric cylindrical shells. Also, Sheng and Wang (2009) used thin piezoelectric layers to investigate the active control of vibration for functionally graded cylindrical shells. Duc *et al*. (2018a) investigated the nonlinear dynamic behavior of FG porous plates resting on elastic foundation under thermal and mechanical loads. The nonlinear thermal dynamic behavior of shear deformable FG plates resting on elastic foundation was studied by Duc *et al*. (2016). Using 1–3 piezoelectric composites, Kumar and Ray (2013) addressed the active control of vibration for analysis of the smart sandwich shells. Duc (2018) presented the nonlinear thermo-electro-mechanical dynamic behavior of shear deformable piezoelectric Sigmoid FG sandwich circular cylindrical shells resting on elastic foundation. Yue *et al.* (2017) experimentally analyzed the active control of vibration for a piezoelectric laminated paraboloidal shell. The active control of vibration for the FG cylindrical shell that reinforced with carbon nanotube using piezoelectric sensor and actuator was investigated by Song *et al.* (2016). Using piezoelectric sensor and actuator, the vibration of shallow doubly curved functionally graded panels was actively controlled by Kiani *et al.* (2013). Using the piezoelectric actuators and sensors, Moita *et al.* (2006) investigated the control of vibration responses for reinforced composite structures. Roy and Chakraborty (2009) used a genetic algorithm to improve the control of vibration for the fiber reinforced polymer composite shell. Jha and Inman (2002) investigated the vibration control analysis of an inflated toroidal shell with piezoelectric patches as actuators and sensors.

In above mentioned studies the influences of stiffeners on the stability and vibration control of systems have not been considered. Some researchers have been focused on the stability and vibration control of stiffened cylindrical shells and plates.

Khoa *et al*. (2019) addressed the nonlinear buckling of imperfect piezoelectric Stiffened FG circular cylindrical shells with metal-ceramic-metal layers under thermal condition. Nonlinear dynamic behavior and vibration analysis of stiffened Stiffened FG elliptical cylindrical shells resting on elastic foundations under thermal condition were studied by Duc *et al*. (2017b). Duc (2013) studied the nonlinear dynamic behavior of imperfect stiffened FG double curved shallow shells resting on elastic foundation. Also, Duc (2016) investigated the nonlinear thermal dynamic behavior of stiffened FG circular cylindrical shells resting on elastic foundations utilizing the theory of Reddy’s third-order shear deformation. Mechanical and thermal stability of stiffened FG conical shell panels resting on elastic foundations under thermal condition was presented by Duc *et al*. (2015). Duc *et al*. (2018b) investigated the nonlinear thermo-mechanical behavior of stiffened Sigmoid FG circular cylindrical shells under compressive and uniform radial loads. Also, Duc *et al*. (2018c) addressed the thermal buckling analysis of FG sandwich truncated conical shells reinforced by FG stiffeners resting on elastic foundation. (Kwak and Yang (2013) used the piezoelectric actuators and sensors to suppress the vibration of the ring-stiffened cylindrical shell subjected to the external fluid. Sohn *et al.* (2014) studied the control of vibration for the reinforced cylindrical shell with ring stiffeners. They used the advanced flexible piezoelectric actuator and derived the governing equation using the finite element method. These researchers considered that the material of stiffeners and shell is isotropic and their control methods are linear.

The literature review reveals that there are no studies on the nonlinear control of SFG cylindrical shells vibration reinforced by internal stiffeners. Therefore, in this study, two nonlinear control strategies consist of sliding mode controller and feedback linearization are developed to suppress the nonlinear vibration of stiffened FG cylindrical shell in the presence of thermal uncertainty. The system is subjected to couple of axial and transverse periodic loads. The nonlinear vibrations of SFG cylindrical shell are controlled by a piezoelectric actuator and sensor. The piezoelectric thin layer actuator is located outside and the ring sensor is attached to inside surface of cylindrical shell. The material composition is considered to be continuously graded in the thickness direction, also these properties depend on temperature. Using the theory of classical shell, smeared stiffeners technique and Galerkin method, the discretized nonlinear differential equations of the system are derived. The effects of stiffeners and different control algorithms such as PID, feedback linearization and sliding mode control on the decreasing the maximum deflection of SFG cylindrical shell are investigated.

2. SFG cylindrical shell with piezoelectric layer

Configuration of the SFG cylindrical shell with thin piezoelectric layer is illustrated in Fig. 1. Coordinate x and $y = R\theta$ represent the axial and the circumferential direction of the cylindrical shell and z for the radial direction (Fig. 1). According to the Fig. 1, the coordinate system (x, y and z) is attached to the left end of middle surface of system. The geometrical of shell L, R and h are axial length, radius and thickness, respectively. For stiffeners s_i, d_i and h_i $(i = r, s)$ are the spacing, width and thickness, respectively. The subscripts r and s refer to ring and stringer stiffeners, respectively. It is considered that the outer surface of shell is metal and the inner surface is ceramic, and for stiffeners it is selected as reverse order. Also, the upper surface of shell is covered by piezoelectric layer with thickness h_p.

3. The theoretical formulation

According to the power law, the volume fractions of the constituents are defined as follows

$$\begin{aligned} &V_c(z) = \left(\frac{2z+h}{2H}\right)^N \; ; \quad H = h,\ h_i\ (i = s,\ r); \ \ N = k,\ K \\ &V_m(z) = 1 - V_c(z) \; ; \ -h/2 \le z \le h/2 \end{aligned} \tag{1}$$

The parameters V_c and V_m denote the ceramic and metal volume fractions and the subscripts *c* and *m* refer to

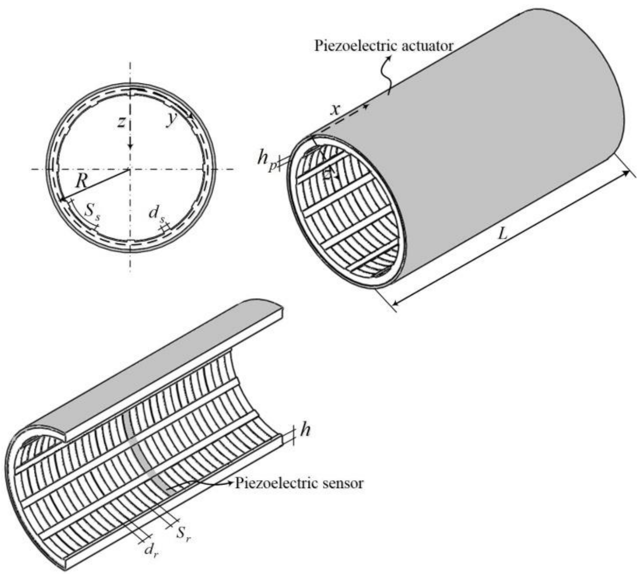

Fig. 1 Configuration of SFG cylindrical shell with piezoelectric layer

the ceramic and metal constituents. $K \geq 0$ and $k \geq 0$ are the material power law index of the FG stiffeners and shell, respectively.

The effective properties P_{eff} can be determined as (Ahmadi and Foroutan 2019, Chen 2018)

$$P_{eff} = P_m(z)V_m(z) + P_c(z)V_c(z) \tag{2}$$

A material coefficient P is defined as a temperature nonlinear function in the following form (Ghiasian *et al*. 2013)

$$P = P_0(P_{-1}T^{-1} + 1 + P_1T + P_2T^2 + P_3T^3) \tag{3}$$

Due to the mentioned law, the mass density and Young's modulus of the shell and stiffeners are defined as follows (Tounsi and Mahmoud 2016, Boukhelf *et al*. 2018)

Shell

$$\begin{gathered} E(z,T) = E_m(T) + \big(E_c(T) - E_m(T)\big)\left(\frac{2z+h}{2h}\right)^k \\ \rho(z,T) =_m (T) + \big(c(T) -_m(T)\big)\left(\frac{2z+h}{2h}\right)^k \\ -\frac{h}{2} \leq z \leq \frac{h}{2} \end{gathered} \tag{4a}$$

Internal stiffener

$$\begin{gathered} E_i(z,T) = E_c(T) + \big(E_m(T) - E_c(T)\big)\left(\frac{2z-h}{2h_i}\right)^K \\ \rho_i(z,T) = \rho_c(T) + \big(\rho_m(T) - \rho_c(T)\big)\left(\frac{2z-h}{2h_i}\right)^K \\ \frac{h}{2} \leq z \leq \frac{h}{2} + h_i\,; \quad i = s, r \end{gathered} \tag{4b}$$

where $\rho_i(z,T)$, $\rho(z,T)$ and $E_i(z,T)$, $E(z,T)$ are the mass density and Young's modulus of the FG stiffeners and shell, respectively.

The strain components are obtained across the thickness of shell at a distance z from the middle surface as follows

$$\begin{gathered} \varepsilon_x = \varepsilon_x^0 - z\chi_x\,, \qquad \varepsilon_y = \varepsilon_y^0 - z\chi_y\,, \\ \gamma_{xy} = \gamma_{xy}^0 - 2z\chi_{xy} \end{gathered} \tag{5}$$

Also, based on the relations of von Kármán strain-displacement (Brush and Almroth 1975), the strain components on the middle surface of shells are given by

$$\begin{aligned} \varepsilon_x^0 &= \frac{\partial u}{\partial x} + \frac{1}{2}\left(\frac{\partial w}{\partial x}\right)^2 \\ \varepsilon_y^0 &= \frac{\partial v}{\partial y} - \frac{w}{R} + \frac{1}{2}\left(\frac{\partial w}{\partial y}\right)^2 \\ \gamma_{xy}^0 &= \frac{\partial u}{\partial y} + \frac{\partial v}{\partial x} + \frac{\partial w}{\partial x}\frac{\partial w}{\partial y} \\ \chi_x &= \frac{\partial^2 w}{\partial x^2}, \quad \chi_y = \frac{\partial^2 w}{\partial y^2}, \quad \chi_{xy} = \frac{\partial^2 w}{\partial x \partial y} \end{aligned} \tag{6}$$

where ε_y^0 and ε_x^0 are the normal strains, and γ_{xy}^0 is the shear strain at the middle surface. $u = u(x,y), v = v(x,y), w = w(x,y)$ are the displacement components along x, y, z axes, respectively. $\chi_x, \chi_y, \chi_{xy}$ are the change of curvatures and twist of shell.

Considering Eq. (6), compatibility equation are given by

$$\begin{aligned} &\frac{\partial^2 \varepsilon_x^0}{\partial y^2} + \frac{\partial^2 \varepsilon_y^0}{\partial x^2} - \frac{\partial^2 \gamma_{xy}^0}{\partial x \partial y} \\ &= -\frac{1}{R}\frac{\partial^2 w}{\partial x^2} + \left(\frac{\partial^2 w}{\partial x \partial y}\right)^2 - \frac{\partial^2 w}{\partial x^2}\frac{\partial^2 w}{\partial y^2} \end{aligned} \tag{7}$$

The relation of stress-strain for FG shell can be written as

$$\begin{Bmatrix} \sigma_x^{sh} \\ \sigma_y^{sh} \\ \tau_{xy}^{sh} \end{Bmatrix} = \begin{bmatrix} A_{11} & A_{12} & 0 \\ A_{12} & A_{11} & 0 \\ 0 & 0 & A_{66} \end{bmatrix} \begin{Bmatrix} \varepsilon_x \\ \varepsilon_y \\ \gamma_{xy} \end{Bmatrix} \tag{8}$$

where

$$A_{11} = \frac{E(z,T)}{1-\nu^2};\ A_{12} = \frac{\nu E(z,T)}{1-\nu^2};\ A_{66} = \frac{E(z,T)}{2(1+\nu)} \tag{9}$$

σ_y^{sh}, σ_x^{sh} and τ_{xy}^{sh} are normal stress in y, x direction and shear stress of un-stiffened shell, respectively and the constant parameter ν is Poisson's ratio.

The relation of stress-strain for FG stiffeners is represented by

$$\begin{Bmatrix} \sigma_s^{st} \\ \sigma_r^{st} \end{Bmatrix} = \begin{bmatrix} E_s & 0 \\ 0 & E_r \end{bmatrix} \begin{Bmatrix} \varepsilon_x \\ \varepsilon_y \end{Bmatrix} \tag{10}$$

where σ_r^{st} and σ_s^{st} are normal stress of the ring and stringer stiffeners, respectively.

3.1 Usage the piezoelectric sensors and actuators

In many recent studies, two common types of piezoelectric materials are widely used (Baillargeon and Vel 2005, Wrona and Pawełczyk 2013), which are piezo-

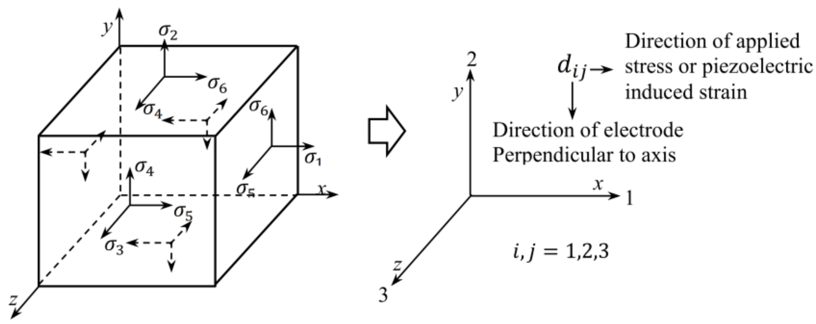

Fig. 2 Directions of the polarization of the piezoelectric material and stress or strain on the vertical planes

polymer, PVDF and piezo-ceramic, PZT. piezo-ceramic can be used both as actuator and sensor but Piezo-polymer are usually utilized as sensor (Hong 1993). The constitutive equation of piezoelectric material for the actuator is given by (Bailey and Hubbard 1985, Fuller *et al.* 1996)

$$\varepsilon_p = S_{pq}^E \sigma_q + d_{pi} E_i^e \tag{11}$$

Also, the dynamic equation of sensor can be expressed as

$$D_i = d_{ip}\sigma_p + \xi_{ij}^{\sigma} E_j^e \tag{12}$$

where $i,j = 1,2,3$ and $q,p = 1,\ldots,6$ as shown in Fig. 2 are directions of polarization of piezoelectric material and strain or stress on the vertical planes, respectively. S_{pq}^E and d_{pi} are the elastic compliance and the piezoelectric strain constant, respectively. ξ is material dielectric permittivity and D_i is electrical displacement.

The stress-strain relations for piezoelectric layer are given by (Song *et al.* 2016)

$$\begin{Bmatrix} \sigma_x^p \\ \sigma_y^p \\ \tau_{xy}^p \end{Bmatrix} = \begin{bmatrix} C_{11} & C_{12} & 0 \\ C_{12} & C_{22} & 0 \\ 0 & 0 & C_{66} \end{bmatrix} \left(\begin{Bmatrix} \varepsilon_x \\ \varepsilon_y \\ \gamma_{xy} \end{Bmatrix} - \begin{bmatrix} 0 & 0 & e_{31} \\ 0 & 0 & e_{32} \\ 0 & 0 & 0 \end{bmatrix} \begin{Bmatrix} 0 \\ 0 \\ \dfrac{V(t)}{h_p} \end{Bmatrix} \right) \tag{13}$$

where

$$C_{11} = \frac{E_p}{1-\nu_p^2}; \quad C_{12} = \frac{\nu_p E_p}{1-\nu_p^2}; \quad C_{66} = \frac{E_p}{2(1+\nu_p)} \tag{14}$$

In Eq. (14), $V(t)$ is the input voltage. ν_p and E_p are the Poisson's ratio and Young's modulus of the piezoelectric material.

Considering the relation of stress-strain of FG shell, stiffeners and piezoelectric layer and then by integrating these equations, the resultant moments and forces for SFG cylindrical shell with piezoelectric layer can be obtained as

Resultant force

$$\begin{Bmatrix} N_x \\ N_y \\ N_{xy} \end{Bmatrix} = \begin{bmatrix} I_{11} & I_{12} & 0 & -J_{11} & -J_{12} & 0 \\ I_{12} & I_{22} & 0 & -J_{12} & -J_{22} & 0 \\ 0 & 0 & I_{33} & 0 & 0 & -2J_{33} \end{bmatrix} \begin{Bmatrix} \varepsilon_x^0 \\ \varepsilon_y^0 \\ \gamma_{xy}^0 \\ \chi_x \\ \chi_y \\ \chi_{xy} \end{Bmatrix} - \begin{Bmatrix} T_1 \\ T_2 \\ 0 \end{Bmatrix} V(t) \tag{15}$$

Resultant moment

$$\begin{Bmatrix} M_x \\ M_y \\ M_{xy} \end{Bmatrix} = \begin{bmatrix} J_{11} & J_{12} & 0 & -K_{11} & -K_{12} & 0 \\ J_{12} & J_{22} & 0 & -K_{12} & -K_{22} & 0 \\ 0 & 0 & J_{33} & 0 & 0 & -2K_{33} \end{bmatrix} \begin{Bmatrix} \varepsilon_x^0 \\ \varepsilon_y^0 \\ \gamma_{xy}^0 \\ \chi_x \\ \chi_y \\ \chi_{xy} \end{Bmatrix} - \begin{Bmatrix} F_1 \\ F_2 \\ 0 \end{Bmatrix} V(t) \tag{16}$$

where J_{ij}, K_{ij} and I_{ij} $(i,j = 1,2,3)$ are the components of the bending, coupling and extensional stiffness of SFG cylindrical shells with piezoelectric layer which are presented in Appendix A. Also, T_i and F_i $(i = 1,2)$ are the external voltage coefficient which are presented in Appendix A. According to Eq. (15), the strain components are rearranged as follows

$$\begin{Bmatrix} \varepsilon_x^0 \\ \varepsilon_y^0 \\ \gamma_{xy}^0 \end{Bmatrix} = \begin{bmatrix} I_{22}^* & -I_{12}^* & 0 & J_{11}^* & J_{12}^* & 0 \\ -I_{12}^* & I_{11}^* & 0 & J_{21}^* & J_{22}^* & 0 \\ 0 & 0 & I_{33}^* & 0 & 0 & 2J_{33}^* \end{bmatrix} \begin{Bmatrix} N_x \\ N_y \\ N_{xy} \\ \chi_x \\ \chi_y \\ \chi_{xy} \end{Bmatrix} + \begin{Bmatrix} T_1^* \\ T_2^* \\ 0 \end{Bmatrix} V(t) \tag{17}$$

Substituting Eq. (17) in Eq. (16) the resultant moments are given by

$$\begin{Bmatrix} M_x \\ M_y \\ M_{xy} \end{Bmatrix} = \begin{bmatrix} J_{22}^* & J_{21}^* & 0 & -K_{11}^* & -K_{12}^* & 0 \\ J_{12}^* & J_{22}^* & 0 & -K_{21}^* & -K_{22}^* & 0 \\ 0 & 0 & J_{33}^* & 0 & 0 & -2K_{33}^* \end{bmatrix} \begin{Bmatrix} N_x \\ N_y \\ N_{xy} \\ \chi_x \\ \chi_y \\ \chi_{xy} \end{Bmatrix} + \begin{Bmatrix} F_1^* \\ F_2^* \\ 0 \end{Bmatrix} V(t) \tag{18}$$

where coefficients I_{ij}^*, J_{ij}^* and K_{ij}^* $(i,j = 1,2,3)$ are presented in Appendix B. Also, coefficients T_i^* and $F_i^*(i = 1,2)$ are presented in Appendix B.

Based on the classical shell theory, the non-linear governing equations of circular shell are as follows (Bich *et al.* 2013, Foroutan *et al.* 2018)

$$\begin{aligned}&\frac{\partial N_x}{\partial x}+\frac{\partial N_{xy}}{\partial y}=0\\&\frac{\partial N_{xy}}{\partial x}+\frac{\partial N_y}{\partial y}=0\\&\frac{\partial^2 M_x}{\partial x^2}+2\frac{\partial^2 M_{xy}}{\partial x\partial y}+\frac{\partial^2 M_y}{\partial y^2}+N_x\frac{\partial^2 w}{\partial x^2}\\&+2N_{xy}\frac{\partial^2 w}{\partial x\partial y}+N_y\left(\frac{\partial^2 w}{\partial y^2}+\frac{1}{R}\right)=\rho_1\frac{\partial^2 w}{\partial t^2}\end{aligned}\tag{19}$$

where t is the time and ρ_1 is the mass density which can be obtained as

$$\rho_1=\left(\rho_m+\frac{\rho_c-\rho_m}{k+1}\right)h+\left(\rho_c+\frac{\rho_m-\rho_c}{K+1}\right)\frac{dh_s}{S}+\rho_p h_p\tag{20}$$

According to the first and second relations of Eq. (19), the resultant forces in term of stress function (φ) are defined as follows

$$N_x=\frac{\partial^2\varphi}{\partial y^2},\ N_y=\frac{\partial^2\varphi}{\partial x^2},\ N_{xy}=-\frac{\partial^2\varphi}{\partial x\partial y}\tag{21}$$

Substituting Eq. (17) in Eqs. (7) and (18) in the third relation of Eq. (19) and according to Eqs. (6) and (21), we yields

$$\begin{aligned}&I_{11}^*\frac{\partial^4\varphi}{\partial x^4}+(I_{33}^*-2I_{12}^*)\frac{\partial^4\varphi}{\partial x^2\partial y^2}+I_{22}^*\frac{\partial^4\varphi}{\partial y^4}+J_{21}^*\frac{\partial^4 w}{\partial x^4}\\&+(J_{11}^*+J_{22}^*-2J_{33}^*)\frac{\partial^4 w}{\partial x^2\partial y^2}+J_{12}^*\frac{\partial^4 w}{\partial y^4}+\frac{1}{R}\frac{\partial^2 w}{\partial x^2}\\&+\left[\left(\frac{\partial^2 w}{\partial x\partial y}\right)^2-\frac{\partial^2 w}{\partial x^2}\frac{\partial^2 w}{\partial y^2}\right]=0\end{aligned}\tag{22}$$

$$\begin{aligned}&\rho_1\frac{\partial^2 w}{\partial t^2}+K_{11}^*\frac{\partial^4 w}{\partial x^4}+(K_{12}^*+K_{21}^*+4K_{33}^*)\frac{\partial^4 w}{\partial x^2\partial y^2}\\&+K_{22}^*\frac{\partial^4 w}{\partial y^4}-J_{21}^*\frac{\partial^4\varphi}{\partial x^4}-(J_{11}^*+J_{22}^*-2J_{33}^*)\frac{\partial^4\varphi}{\partial x^2\partial y^2}\\&-J_{12}^*\frac{\partial^4\varphi}{\partial y^4}-\frac{1}{R}\frac{\partial^2\varphi}{\partial x^2}-\frac{\partial^2\varphi}{\partial y^2}\frac{\partial^2 w}{\partial x^2}+2\frac{\partial^2\varphi}{\partial x\partial y}\frac{\partial^2 w}{\partial x\partial y}\\&-\frac{\partial^2\varphi}{\partial x^2}\frac{\partial^2 w}{\partial y^2}+\frac{\partial^2 M_x^p}{\partial x^2}+\frac{\partial^2 M_y^p}{\partial y^2}=0\end{aligned}\tag{23}$$

In Eq. (23), M_y^p and M_x^p, are the actuator induced bending moment. When piezoelectric is subjected to external loads, charges are produced on the sensor as follows (Song *et al.* 2016)

$$Q_s(t)=\widehat{K}_s W(t)\tag{24}$$

where $\widehat{K}_s$ is coefficient matrix. The voltage for sensor ($V_s(t)$) is defined as

$$V_s(t)=\frac{h_p}{\Xi_{33}A_s}Q_s(t)\tag{25}$$

where Ξ_{33} is the dielectric constant and A_s is the sensor surface area.

Substituting Eq. (24) into Eq. (25) as follows

$$V_s(t)=\frac{h_p}{\Xi_{33}A_s}\widehat{K}_s W(t)\tag{26}$$

3.2 Boundary conditions

A simply supported SFG cylindrical shell under the couple of transverse and axial periodic loads is considered. The applied boundary conditions are the following form

$$\begin{aligned}&w=0;\quad M_x=0;\quad N_x=-P_x h,\\&N_y=-P_y h;\quad N_{xy}=0;\quad at\quad x=0,\ L\end{aligned}\tag{27}$$

Due to above boundary condition, the proposed approximate solution of deflection is considered as (Foroutan *et al.* 2018, Volmir 1972)

$$w=W(t)\sin\frac{m\pi x}{L}\sin\frac{ny}{R}\tag{28}$$

In Eq. (28), $W(t)$ is time dependent amplitude, n and m are the number of full and half wave in the circumferential and axial directions, respectively.

Eq. (28) is substituted in Eq. (22) and then the resultant equation is solved to find the unknown stress function (φ) as follows

$$\begin{aligned}\varphi=&F_1\cos\frac{2m\pi x}{L}+F_2\cos\frac{2ny}{R}\\&-F_3\sin\frac{m\pi x}{L}\sin\frac{ny}{R}-P_x h\frac{y^2}{2}-P_y h\frac{x^2}{2}\end{aligned}\tag{29}$$

where P_y and P_x are the average circumferential and axial stresses, respectively. Also, the coefficients $F_i(i=1,2,3)$ are in the following form

$$\begin{aligned}F_1&=\frac{n^2\lambda^2}{32J_{11}^*m^2\pi^2}W(t)^2\\F_2&=\frac{m^2\pi^2}{32J_{22}^*n^2\lambda^2}W(t)^2\\F_3&=\frac{B}{A}W(t)\end{aligned}\tag{30}$$

where coefficients A and B are presented in Appendix B.

Eqs. (28)-(30) are substituted in Eq. (23) and then the Galerkin method is applied to obtain the discretized equation as follows

$$\begin{aligned}&\ddot{W}+a_1W+a_2W^3-a_3P_XW\\&-a_4P_yW+a_5V(t)=0\end{aligned}\tag{31}$$

In the Eq. (31), $a_i\ (i=1,\ldots,5)$ are defined in appendix B.

3.3 Free vibration analysis

To analyze the free vibration of SFG cylindrical shell, the controller, periodic loads and nonlinear term (W^3) in

Eq. (31) are ignored. Thus, Eq. (31) reduces to

$$\frac{\partial^2 w}{\partial t^2} + a_1 w = 0 \quad (32)$$

According to Eq. (32), natural frequencies for the SFG cylindrical shell are obtained as

$$\omega_n = \sqrt{a_1} \quad (33)$$

3.4 Control strategy formulation

A linear and two nonlinear control methods are utilized to suppress the nonlinear vibration of SFG cylindrical shell. These control methods are as follows: (1) PID control method, (2) feedback linearization and (3) sliding mode control, which are design in order to compare with PID control method.

3.4.1 PID controller

A proportional–integral–derivative controller (PID controller) is a control loop feedback mechanism that is widely used in industrial control systems. A PID controller continuously calculates an error value ($e(t)$) and applies a correction based on proportional, integral, and derivative terms (denoted P, I and D, respectively). The control law of PID controller is expressed as (Ogata and Yang 2002)

$$V(t) = K_p e(t) + K_i \int e(t)dt + K_d \dot{e}(t) \quad (34)$$

where K_i, K_d and K_p are the integral, derivative and proportional gains, respectively.

3.4.2 Feedback linearization strategy

A common well-known approach that is used in the control of nonlinear plants, is feedback linearization. Using this controller, the nonlinear models are transformed into linear ones. With regard to Eq. (31), feedback linearization control is considered as follows

$$V(t) = \frac{1}{a_5}\left[-a_1 W - a_2 W^3 + \ddot{W}_d + K_p e(t) + K_d \dot{e}(t)\right] \quad (35)$$

To prove the stability of proposed controller, Eq. (35) is substituted into Eq. (31) and then the closed loop system is obtained as

$$\frac{1}{a_5}\left[\ddot{W} + K_d \dot{e}(t) + K_p e(t)\right] = -a_3 P_X W - a_4 P_y W \quad (36)$$

Because of the $W_d(t) = \dot{W}_d(t) = \ddot{W}_d(t) = 0$, then $e(t) = W(t)$, $\dot{e}(t) = \dot{W}(t)$, $\ddot{e}(t) = \ddot{W}(t)$. Therefore, according to Eq. (36), the error dynamic is simplified as

$$\ddot{e} + K_d \dot{e}(t) + \left[K_p - a_5\left(a_3 P_X + a_4 P_y\right)\right]e(t) = 0 \quad (37)$$

With regard to Eq. (37), for closed loop system stability, K_d and K_p must be considered as follows

$$K_d > 0 \quad and \quad K_p > a_5\left(a_3 P_X + a_4 P_y\right) \quad (38)$$

3.4.3 Sliding mode controller

Because of the system is in presence of thermal uncertainty, A robust control strategy should be used. The sliding mode algorithm is the one of the robust control methods that this method is utilized to control of system. For this purpose, first, Eq. (31) is changed in the following form

$$\ddot{W} + F = gV(t) \quad (39)$$

where

$$F = a_1 W + a_2 W^3 - a_3 P_X W - a_4 P_y W; \quad g = -a_5 \quad (40)$$

In Eq. (39), F is unknown dynamics, but estimated of that $\hat{f}$ is assumed known. The bound of ΔF i.e., H is assumed known function as follows

$$F = \hat{f} + \Delta F; \quad \Delta F = F - \hat{f} \le H \quad (41)$$

To control of system using the sliding method, we define the Sliding surface i.e., S as

$$S = \dot{e} + \lambda e \quad (42)$$

According to method of sliding mode control, in order to stability of system, sliding surface must be satisfy the following condition

$$\dot{S}\mathrm{sgn}(S) \le -\eta \quad (43)$$

By considering $\ddot{e}(t) = \ddot{W}(t)$ and according to Eq. (39), Eq. (42) and its derivative substitute into (43), yields

$$\left(\hat{f} + \Delta F - gV(t) + \lambda\dot{e}\right)\mathrm{sgn}(S) \le -\eta \quad (44)$$

To compensate for the uncertainties, the controller law is proposed as follows

$$gV(t) = \hat{f} + \lambda\dot{e} + U\mathrm{sgn}(S) \quad (45)$$

U is defined such that satisfy the Eq. (44). Substituting Eq.(45) into Eq. (44) and according to Eq. (41), we yields

$$U = \eta + H \quad (46)$$

Finally, by substituting Eq. (46) into Eq. (45), the sliding mode control for SFG cylindrical shell is obtained as

$$gV(t) = \hat{f} + \lambda\dot{e} + (\eta + H)\mathrm{sgn}(S) \quad (47)$$

4. Numerical results

4.1 Validation of the present approach

For validating the present approach, in Table 1, the natural frequencies of simply supported cylindrical shell presented in this work is considered in comparison with the (Pellicano 2007) and (Qin *et al.* 2017) results. The differences between present results and the literature are less than 0.8%. Also, in Table 2, the natural frequencies of SFG cylindrical shell for our study are compared with the obtained natural frequencies by (Dung and Nam 2014). So, comparisons show that the good conformance is obtained.

In Figs. 3 and 4, the natural frequencies of the cylindrical shells for the various number of full waves without stiffeners and with internal stiffeners are compared with those of Sewall and Naumann (1968) and Sewall *et al*. (1964). They experimentally analyzed the vibration response of the cylindrical shells. These comparisons also show that good agreements are obtained.

4.2 Vibration response of stiffened FG cylindrical shell

Here, the vibration for SFG cylindrical shell with piezoelectric layer is analyzed. The influence of material parameters and different geometrical such as internal stiffeners, volume fraction of FG, the effect of periodic load and different control algorithms on nonlinear vibration responses of SFG cylindrical shells are considered. The number of stiffeners is assumed considered to be thirty. The FG cylindrical shell is considered to be made of SUS304 (Metal) and Si_3N_4 (Ceramic). Table 3 shows the material properties for FG cylindrical shells.

Table 1 Comparison of the natural frequencies of simply supported ($L = 0.2$ m, $R = 0.1$ m, $h = 0.247 \times 10^{-3}$ m, $m = 1, \nu = 0.31, E = 7.12 \times 10^{10}$ N/m^2, $\rho = 2796$ kg/m^3)

m	n	Present	(Qin *et al.* 2017)		(Pellicano 2007)	
				Errors (%)		Errors (%)
1	7	486.0	484.6	0.2	484.6	0.2
1	8	490.3	489.6	0.1	489.6	0.1
1	9	545.8	546.2	0.07	546.2	0.07
1	6	555.8	553.3	0.4	553.3	0.4
1	10	634.8	636.8	0.3	636.8	0.3
1	5	728.5	722.1	0.8	722.1	0.8
1	11	746.6	750.7	0.5	750.7	0.5
1	12	875.5	882.2	0.7	882.2	0.7
2	10	962.3	968.1	0.5	968.1	0.5
2	11	976.6	983.4	0.6	983.4	0.6

Table 2 Comparison of the natural frequencies of SFG cylindrical shell ($L = 0.75$ m, $R = 0.5$ m, $R/h = 250$, $m = 1$, $E_m = 7 \times 10^{10}$ N/m^2, $h_s = h_r = 0.01$ m, $\rho_m = 2702$ kg/m^3, $E_c = 38 \times 10^{10}$ N/m^2, $\rho_c = 3800$ kg/m^3, $\nu = 0.3, d_s = d_r = 0.0025$ m)

Present	(Dung and Nam 2014)	Errors (%)
	Un-stiffened	
1654.05	1654.05	0.00
	Internal stiffeners	
2539.43	2539.43	0.00

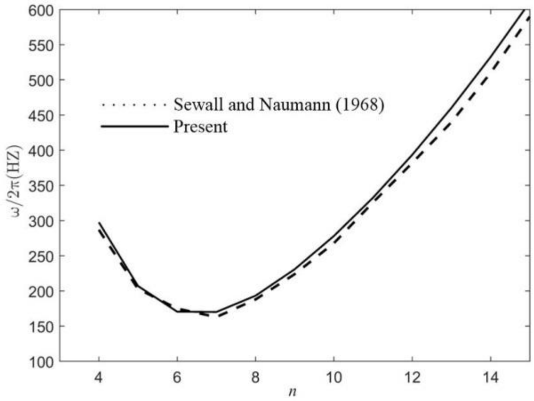

Fig. 3 Comparison of the natural frequencies of isotropic cylindrical shells without stiffeners ($m = 1$)

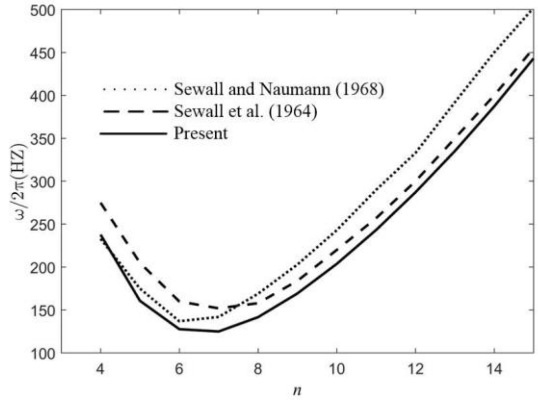

Fig. 4 Comparison of the natural frequencies of isotropic cylindrical shells with internal stiffeners ($m = 1$)

The Poisson's ratio for ceramic, metal and piezoelectric is considered to be equal (i.e., $\nu = \nu_m = \nu_c = \nu_p$). The rest of material parameters and geometrical characteristics of system are listed in Table 4.

The effect of stiffeners on vibration response of the FG cylindrical shell is illustrated in Fig. 5. Considering Fig. 5, the stiffeners strongly decrease the maximum deflection of FG cylindrical shell.

The influence of material properties of the FG stiffeners and shell without piezoelectric layer on the vibration behavior is shown in Table 4. Due to this table, metallic shell with metallic stiffeners and ceramic shell with ceramic

Table 3 Material properties of the constituent materials of the considered FG cylindrical shells (Duc and Thang 2015)

Present	(Dung and Nam 2014)	Errors (%)
	Un-stiffened	
1654.05	1654.05	0.00
	Internal stiffeners	
2539.43	2539.43	0.00

Table 4 The geometrical and material parameters of system

Material parameters	Value	Geometrical characteristics	Value
E_p	63 GPa	R	0.5 m
ρ_m	$2702\ \mathrm{kg/m^3}$	L	0.75 m
ρ_c	$3800\ \mathrm{kg/m^3}$	h	0.002 m
ρ_p	$7600\ \mathrm{kg/m^3}$	h_s	0.01 m
ν	0.3	d	0.0025 m
$e_{31}=e_{32}$	$245\times10^{-12}\ \mathrm{mV^{-1}}$	h_p	0.002 m
Ξ_{33}	$1.5\times10^{-8}\ \mathrm{Fm^{-1}}$	m, n	1, 5

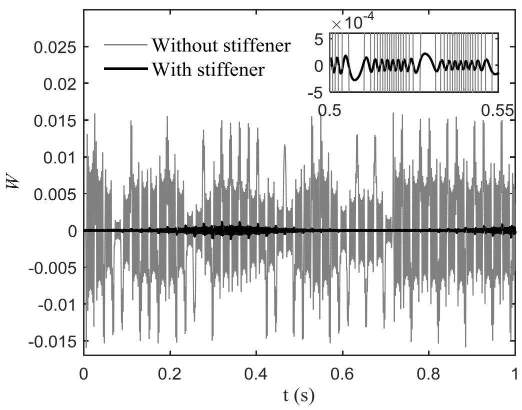

Fig. 5 Effect of stiffeners on vibration response of FG cylindrical shell

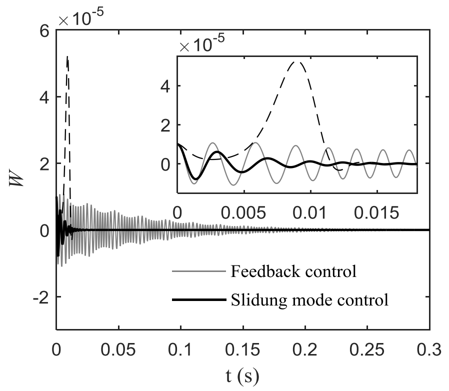

Fig. 6 Effect of stiffeners on vibration response of FG cylindrical shell

Table 5 Effect of material properties on the maximum deflection of vibration response of SFG cylindrical shell without piezoelectric layer ($\times 10^{-3}$m)

	Type of stiffeners		
	Ceramic	FGM	Metal
Ceramic shell	0.000014	0.000016	0.000018
FGM shell	0.000016	0.0011	0.000016
Metal shell	0.000043	0.0091	0.0107

stiffeners have the lowest and the highest resistance against the nonlinear vibration response, respectively.

Fig. 6 shows the effect of different controls such as PID, feedback and sliding mode on the response of nonlinear vibration for FG cylindrical shell without stiffeners under uncertainty. Due to this figure, sliding mode and PID control have the most and least effect on decreasing the maximum deflection of nonlinear vibration of cylindrical shell. Actuator voltage of PID, feedback and sliding mode control is shown in Fig. 7. According to this figure, the range of maximum actuator voltage of the three controllers is almost at the same level.

The influence of different temperatures on the SFG cylindrical shell vibration is demonstrated in Fig. 8. As can be seen, generally increasing the temperature leads to increasing the maximum deflection of SFG cylindrical shell.

The effect of various controllers on the response of nonlinear vibration for stiffened and un-stiffened FG shell is illustrated in Fig. 9. With regard to Fig. 9, the effect of feedback and sliding mode controls on decreasing the maximum deflection of cylindrical shell without stiffener is more than one with stiffener. But the effect of PID control on decreasing the maximum deflection of cylindrical shell without stiffener much less than one with stiffener.

5. Conclusions

Active control of nonlinear vibration of stiffened functionally graded (SFG) cylindrical shell is studied in this study. Different control algorithms are applied to SFG shell in presence of thermal uncertainty for investigation of vibration reduction. The material composition is considered to be continuously graded in the thickness direction,

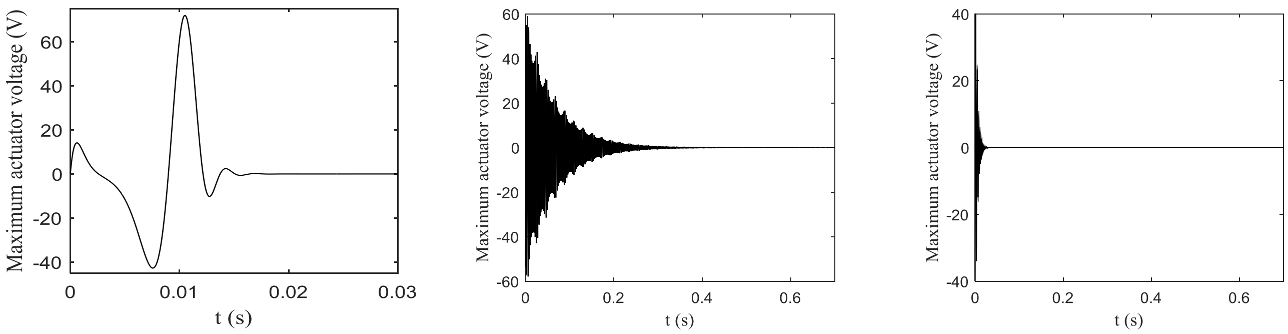

(a) PID control (b) Feedback control (c) Sliding mode control

Fig. 7 Maximum actuator voltage of controllers

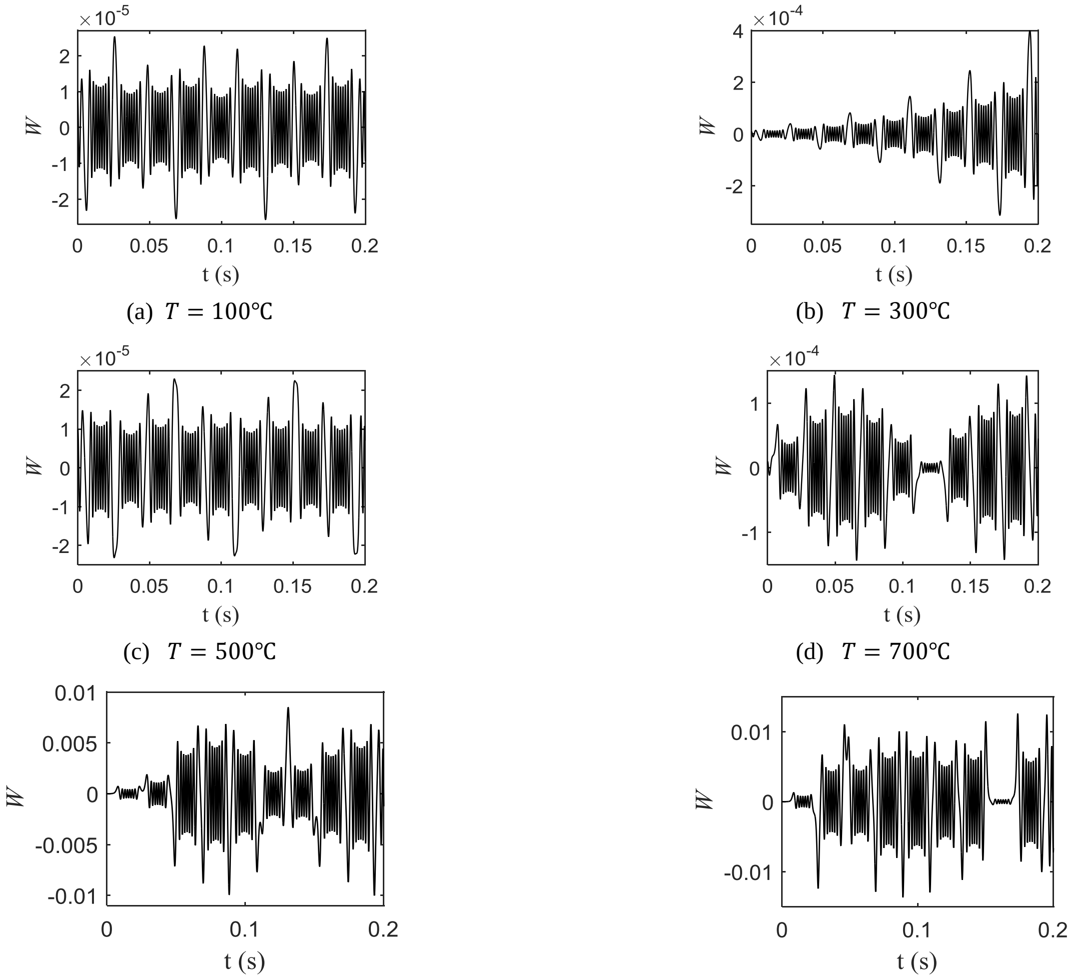

(a) $T = 100℃$ (b) $T = 300℃$

(c) $T = 500℃$ (d) $T = 700℃$

(e) $T = 900℃$ (f) $T = 1100℃$

Fig. 8 Effect of different temperatures on the vibration response of SFG cylindrical shell

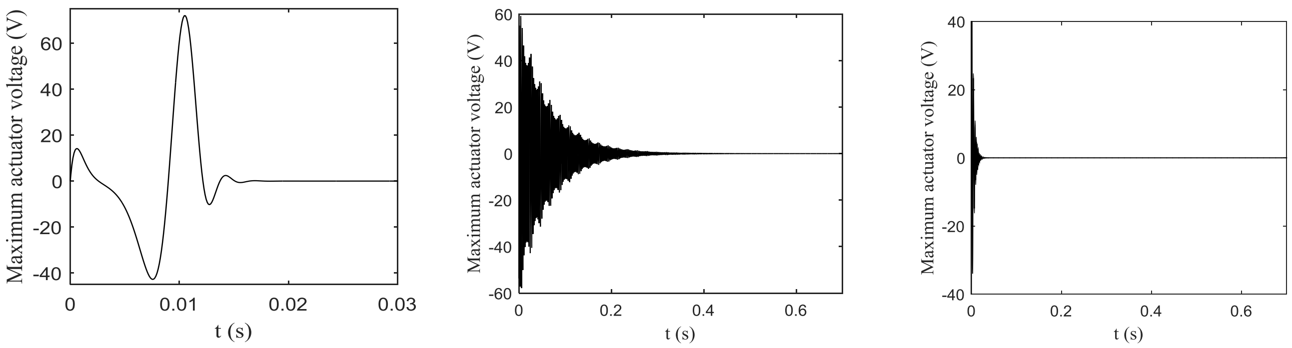

(a) PID control (b) Feedback control (c) Sliding mode control

Fig. 9 Maximum actuator voltage of controllers

also these properties varies with temperature. The inner surface of SFG cylindrical shell reinforced by eccentrically stringer and ring stiffeners and outer surface of shell is covered by the piezoelectric layer. Using the theory of classical shell, smeared stiffeners technique and Galerkin method, the discretized nonlinear differential equations of system are derived. The effects of stiffeners and various controls such as PID, feedback and sliding mode on the response of nonlinear vibration for SFG cylindrical shells are examined and the following conclusions are obtained

- The stiffeners strongly decrease the maximum deflection of FG cylindrical shell.
- Generally increasing the temperature leads to increasing the maximum deflection of SFG cylindrical shell.

- Metallic shell with metallic stiffeners and Ceramic shell with ceramic stiffeners have the lowest and highest the resistance against the nonlinear vibration response, respectively.
- Sliding mode and PID control have the most and least effect on decreasing the maximum deflection of cylindrical shell vibration.
- The influence of feedback and sliding mode controls on decreasing the maximum deflection of cylindrical shell with stiffener is more than cylindrical shell without stiffener.
- Sliding mode controller is more effective than other controllers on the vibration reduction in presence of uncertainty.

References

Ahmadi, H. and Foroutan, K. (2019), "Nonlinear primary resonance of spiral stiffened functionally graded cylindrical shells with damping force using the method of multiple scales", *Thin-Wall Struct*., **135**, 33-44. https://doi.org/10.1016/j.tws.2018.10.028

Bailey, T. and Hubbard, J.E. (1985), "Distributed piezoelectric-polymer active vibration control of a cantilever beam", *J. Guidance Control Dyn*., **8**(5), 605-611. https://doi.org/10.2514/3.20029

Baillargeon, B.P. and Vel, S.S. (2005), "Active vibration suppression of sandwich beams using piezoelectric shear actuators: Experiments and numerical simulations", *J. Intell. Mater. Syst. Struct*., **16**(6), 517-530. https://doi.org/10.1177/1045389X05053154

Bich, D.H., Van Dung, D., Nam, V.H. and Phuong, N.T. (2013), "Nonlinear static and dynamic buckling analysis of imperfect eccentrically stiffened functionally graded circular cylindrical thin shells under axial compression", *Int. J. Mech. Sci*., **74**, 190-200. https://doi.org/10.1016/j.ijmecsci.2013.06.002

Biglar, M., Mirdamadi, H.R. and Danesh, M. (2014), "Optimal locations and orientations of piezoelectric transducers on cylindrical shell based on gramians of contributed and undesired rayleigh–ritz modes using genetic algorithm", *J. Sound Vib*., **333**(5), 1224-1244. https://doi.org/10.1016/j.jsv.2013.10.025

Boukhelf, F., Bouiadjra, M.B., Bouremana, M. and Tounsi, A. (2018), "Hygro-thermo-mechanical bending analysis of FGM plates using a new HSDT", *Smart Struct. Syst., Int. J*., **21**(1), 75-97. https://doi.org/10.12989/sss.2018.21.1.075

Brush, D.O. and Almroth, B.O. (1975), *Buckling of Bars, Plates, and Shells*, McGraw-Hill New York, NY, USA.

Chen, Y.Z. (2018), "Transfer matrix method for solution of FGMs thick-walled cylinder with arbitrary inhomogeneous elastic response", *Smart Struct. Syst., Int. J*., **21**(4), 469-477. https://doi.org/10.12989/sss.2018.21.4.469

Cong, P.H., Chien, T.M., Khoa, N.D. and Duc, N.D. (2018), "Nonlinear thermomechanical buckling and post-buckling response of porous FGM plates using Reddy's HSDT", *Aerosp. Sci. Technol*., **77**, 419-428. https://doi.org/10.1016/j.ast.2018.03.020

Correia, I.P., Soares, C.M.M., Soares, C.A.M. and Herskovits, J. (2002), "Active control of axisymmetric shells with piezoelectric layers: A mixed laminated theory with a high order displacement field", *Comput. Struct*., **80**(27-30), 2265-2275. https://doi.org/10.1016/S0045-7949(02)00239-0

Duc, N.D. (2013), "Nonlinear dynamic response of imperfect eccentrically stiffened FGM double curved shallow shells on elastic foundation", *Compos. Struct*., **99**, 88-96. https://doi.org/10.1016/j.compstruct.2012.11.017

Duc, N.D. (2016), "Nonlinear thermal dynamic analysis of eccentrically stiffened S-FGM circular cylindrical shells surrounded on elastic foundations using the Reddy's third-order shear deformation shell theory", *Eur. J. Mech. A-Solid*., **58**, 10-30. https://doi.org/10.1016/j.euromechsol.2016.01.004

Duc, N.D. (2018), "Nonlinear thermo-electro-mechanical dynamic response of shear deformable piezoelectric sigmoid functionally graded sandwich circular cylindrical shells on elastic foundations", *J. Sandw. Struct. Mater*., **20**(3), 351-378. https://doi.org/10.1177/1099636216653266

Duc, N.D. and Cong, P.H. (2018), "Nonlinear dynamic response and vibration of sandwich composite plates with negative Poisson's ratio in auxetic honeycombs", *J. Sandw. Struct. Mater*., **20**(6), 692-717. https://doi.org/10.1177/1099636216674729

Dung, D. and Nam, V.H. (2014), "Nonlinear dynamic analysis of eccentrically stiffened functionally graded circular cylindrical thin shells under external pressure and surrounded by an elastic medium", *Eur. J. Mech. A-Solid*., **46**, 42-53. https://doi.org/10.1016/j.euromechsol.2014.02.008

Duc, N.D. and Thang, P.T. (2015), "Nonlinear dynamic response and vibration of shear deformable imperfect eccentrically stiffened s-fgm circular cylindrical shells surrounded on elastic foundations", *Aerosp. Sci. Technol*., **40**, 115-127. https://doi.org/10.1016/j.ast.2014.11.005

Duc, N.D., Anh, V.T.T. and Cong, P.H. (2014), "Nonlinear axisymmetric response of FGM shallow spherical shells on elastic foundations under uniform external pressure and temperature", *Eur. J. Mech. A-Solid*., **45**, 80-89. https://doi.org/10.1016/j.euromechsol.2013.11.008

Duc, N.D., Cong, P.H., Anh, V.M., Quang, V.D., Tran, P., Tuan, N.D. and Thinh, N.H. (2015), "Mechanical and thermal stability of eccentrically stiffened functionally graded conical shell panels resting on elastic foundations and in thermal environment", *Compos. Struct*., **132**, 597-609. https://doi.org/10.1016/j.compstruct.2015.05.072

Duc, N.D., Bich, D.H. and Cong, P.H. (2016), "Nonlinear thermal dynamic response of shear deformable FGM plates on elastic foundations", *J. Therm. Stress*., **39**(3), 278-297.

Duc, N.D., Lee, J., Nguyen-Thoi, T. and Thang, P.T. (2017a), "Static response and free vibration of functionally graded carbon nanotube-reinforced composite rectangular plates resting on Winkler–Pasternak elastic foundations", *Aerosp. Sci. Technol*., **68**, 391-402. https://doi.org/10.1016/j.ast.2017.05.032

Duc, N.D., Nguyen, P.D. and Khoa, N.D. (2017b), "Nonlinear dynamic analysis and vibration of eccentrically stiffened S-FGM elliptical cylindrical shells surrounded on elastic foundations in thermal environments", *Thin Wall Struct*., **117**, 178-189. https://doi.org/10.1016/j.tws.2017.04.013

Duc, N.D., Quang, V.D., Nguyen, P.D. and Chien, T.M. (2018a), "Nonlinear dynamic response of functionally graded porous porous plates on elastic foundation subjected to thermal and mechanical loads using the first order shear deformation theory", *J. Appl. Comput. Mech*., **4**(4), 245-259. https://doi.org/10.22055/JACM.2018.23219.1151

Duc, N.D., Khoa, N.D. and Thiem, H.T. (2018b), "Nonlinear thermo-mechanical response of eccentrically stiffened Sigmoid FGM circular cylindrical shells subjected to compressive and uniform radial loads using the Reddy's third-order shear deformation shell theory", *Mech. Adv. Mater. Struct*., **25**(13), 1156-1167. https://doi.org/10.1080/15376494.2017.1341581

Duc, N.D., Kim, S.E. and Chan, D.Q. (2018c), "Thermal buckling analysis of FGM sandwich truncated conical shells reinforced by FGM stiffeners resting on elastic foundations using FSDT", *J Therm. Stress*., **41**(3), 331-365. https://doi.org/10.1080/01495739.2017.1398623

Duc, N.D., Hadavinia, H., Quan, T.Q. and Khoa, N.D. (2019), "Free vibration and nonlinear dynamic response of imperfect nanocomposite FG-CNTRC double curved shallow shells in thermal environment", *Eur. J. Mech. A-Solid.*, **75**, 355-366. https://doi.org/10.1016/j.compstruct.2015.05.072

Foroutan, K., Shaterzadeh, A. and Ahmadi, H. (2018), "Nonlinear dynamic analysis of spiral stiffened functionally graded cylindrical shells with damping and nonlinear elastic foundation under axial compression", *Struct. Eng. Mech., Int. J.*, **66**(3), 295-303. https://doi.org/10.12989/sem.2018.66.3.295

Fuller, C.C., Elliott, S. and Nelson, P.A. (1996), *Active Control of Vibration*, Academic Press.

Ghiasian, S., Kiani, Y. and Eslami, M. (2013), "Dynamic buckling of suddenly heated or compressed fgm beams resting on nonlinear elastic foundation", *Compos. Struct.*, **106**, 225-234. https://doi.org/10.1016/j.compstruct.2013.06.001

Hasheminejad, S.M. and Oveisi, A. (2016), "Active vibration control of an arbitrary thick smart cylindrical panel with optimally placed piezoelectric sensor/actuator pairs", *Int. J. Mech. Mater. Des.*, **12**(1), 1-16. https://doi.org/10.1007/s10999-015-9293-2

Hong, S.Y. (1993), "Active vibration control of adaptive flexible structures using piezoelectric smart sensors and actuators", *J. Acoust. Soc. Am.*, **93**(2), 1205-1205. https://doi.org/10.1121/1.405523

Jha, A. and Inman, D. (2002), "Piezoelectric actuator and sensor models for an inflated toroidal shell", *Mech. Syst. Signal Pr.*, **16**(1), 97-122. https://doi.org/10.1006/mssp.2001.1442

Khoa, N.D., Thiem, H.T. and Duc, N.D. (2019), "Nonlinear buckling and postbuckling of imperfect piezoelectric S-FGM circular cylindrical shells with metal–ceramic–metal layers in thermal environment using Reddy's third-order shear deformation shell theory", *Mech. Adv. Mater. Struct.*, **26**(3), 248-259. https://doi.org/10.1080/15376494.2017.1341583

Kiani, Y., Sadighi, M. and Eslami, M. (2013), "Dynamic analysis and active control of smart doubly curved FGM panels", *Compos. Struct.*, **102**, 205-216. https://doi.org/10.1016/j.compstruct.2013.02.031

Kim, S.J., Hwang, J.S., Mok, J. and Ko, H.M. (2001), "Active vibration control of composite shell structure using modal sensor/actuator system", *Smart. Struct. Integr. Syst.*, **4327**, 688-697. https://doi.org/10.1117/12.436576

Kumar, R.S. and Ray, M. (2013), "Active control of geometrically nonlinear vibrations of doubly curved smart sandwich shells using 1–3 piezoelectric composites", *Compos. struct.*, **105**, 173-187. https://doi.org/10.1016/j.compstruct.2013.03.010

Kwak, M.K. and Yang, D.-H. (2013), "Active vibration control of a ring-stiffened cylindrical shell in contact with unbounded external fluid and subjected to harmonic disturbance by piezoelectric sensor and actuator", *J. Sound Vib.*, **332**(20), 4775-4797. https://doi.org/10.1016/j.jsv.2013.04.014

Kwak, M.K., Heo, S. and Jeong, M. (2009), "Dynamic modelling and active vibration controller design for a cylindrical shell equipped with piezoelectric sensors and actuators", *J. Sound Vib.*, **321**(3-5), 510-524. https://doi.org/10.1016/j.jsv.2008.09.051

Kwak, M.K., Yang, D.-H. and Lee, J.-H. (2012), "Active vibration control of a submerged cylindrical shell by piezoelectric sensors and actuatorsed", *Int. Soc. Optics Photon.*, **8341**, 83412F. https://doi.org/10.1117/12.916032

Loghmani, A., Danesh, M., Kwak, M.K. and Keshmiri, M. (2017), "Vibration suppression of a piezo-equipped cylindrical shell in a broad-band frequency domain", *J. Sound Vib.*, **411**, 260-277. https://doi.org/10.1016/j.jsv.2017.08.051

Ma, X., Jin, G. and Liu, Z. (2014), "Active structural acoustic control of an elastic cylindrical shell coupled to a two-stage vibration isolation system", *Int. J. Mech. Sci.*, **79**, 182-194. https://doi.org/10.1016/j.ijmecsci.2013.12.010

Moita, J.M.S., Correia, V.M.F., Martins, P.G., Soares, C.M.M. and Soares, C.A.M. (2006), "Optimal design in vibration control of adaptive structures using a simulated annealing algorithm", *Compos. Struct.*, **75**(1-4), 79-87. https://doi.org/10.1016/j.compstruct.2006.04.062

Ogata, K. and Yang, Y. (2002), *Modern Control Engineering*, Prentice Hall, India.

Pan, X. and Hansen, C. (1997), "Active control of vibration transmission in a cylindrical shell", *J. Sound Vib.*, **203**(3), 409-434. https://doi.org/10.1006/jsvi.1996.9987

Pellicano, F. (2007), "Vibrations of circular cylindrical shells: Theory and experiments", *J. Sound Vib.*, **303**(1-2), 154-170. https://doi.org/10.1016/j.jsv.2007.01.022

Plattenburg, J., Dreyer, J.T. and Singh, R. (2017), "Vibration control of a cylindrical shell with concurrent active piezoelectric patches and passive cardboard liner", *Mech. Syst. Signal Pr.*, **91**, 422-437. https://doi.org/10.1016/j.ymssp.2016.11.008

Qin, Z., Chu, F. and Zu, J. (2017), "Free vibrations of cylindrical shells with arbitrary boundary conditions: A comparison study", *Int. J. Mech. Sci.*, **133**, 91-99. https://doi.org/10.1016/j.ijmecsci.2017.08.012

Roy, T. and Chakraborty, D. (2009), "Optimal vibration control of smart fiber reinforced composite shell structures using improved genetic algorithm", *J. Sound Vib.*, **319**(1-2), 15-40. https://doi.org/10.1016/j.jsv.2008.05.037

Sewall, J.L. and Naumann, E.C. (1968), "An experimental and analytical vibration study of thin cylindrical shells with and without longitudinal stiffeners", NASA TN D-4705.

Sewall, J.L., Clary, R.R. and Leadbetter, S.A. (1964), "An experimental and analytical vibration study of a ring-stiffened cylindrical shell structure with various support conditions", NASA TN D-2398.

Sheng, G. and Wang, X. (2009), "Active control of functionally graded laminated cylindrical shells", *Compos. Struct.*, **90**(4), 448-457. https://doi.org/10.1016/j.compstruct.2010.06.007

Sheng, G. and Wang, X. (2010), "Response and control of functionally graded laminated piezoelectric shells under thermal shock and moving loadings", *Compos. Struct.*, **93**(1), 132-141. https://doi.org/10.1016/j.compstruct.2010.06.007

Sohn, J.W., Jeon, J. and Choi, S.-B. (2014), "Active vibration control of ring-stiffened cylindrical shell structure using macro fiber composite actuators", *J. Nanosci. Nanotechno.*, **14**(10), 7526-7532. https://doi.org/10.1166/jnn.2014.9748

Song, Z., Zhang, L. and Liew, K. (2016), "Active vibration control of cnt-reinforced composite cylindrical shells via piezoelectric patches", *Compos. Struct.*, **158**, 92-100. https://doi.org/10.1016/j.compstruct.2016.09.031

Tan, X. and Vu-Quoc, L. (2005), "Optimal solid shell element for large deformable composite structures with piezoelectric layers and active vibration control", *Int. J. Numer. Meth. Eng.*, **64**(15), 1981-2013. https://doi.org/10.1002/nme.1433

Thom, D.V., Kien, N.D., Duc, N.D., Duc, D.H. and Tinh, B.Q. (2017), "Analysis of bi-directional functionally graded plates by FEM and a new third-order shear deformation plate theory", *Thin-Wall. Struct.*, **119**, 687-699. https://doi.org/10.1016/j.tws.2017.07.022

Tounsi, A. and Mahmoud, S.R. (2016), "Hygro-thermo-mechanical bending of S-FGM plates resting on variable elastic foundations using a four-variable trigonometric plate theory", *Smart Struct. Syst., Int. J.*, **18**(4), 755-786. https://doi.org/10.12989/sss.2016.18.4.755

Volmir, A.S. (1972), *Non-linear Dynamics of Plates and Shells*, Science Edition M, USSR.

Wrona, S. and Pawełczyk, M. (2013), "Controllability-oriented placement of actuators for active noise-vibration control of rectangular plates using a memetic algorithm", *Arch. Acoust.*,

38(4), 529-536. https://doi.org/10.2478/aoa-2013-0062
Yue, H., Lu, Y., Deng, Z. and Tzou, H. (2017), "Experiments on vibration control of a piezoelectric laminated paraboloidal shell", *Mech. Syst. Signal Pr.*, **82**, 279-295. https://doi.org/10.1016/j.ymssp.2016.05.023

HJ

Appendix A

$$\begin{aligned}
&I_{11} = \frac{E_1}{1-\nu^2} + \frac{E_{1S} d_s}{S_s}; \quad I_{22} = \frac{E_1}{1-\nu^2} + \frac{E_{1r} d_r}{S_r} \\
&I_{12} = \frac{E_1 \nu}{1-\nu^2}; \quad I_{33} = \frac{E_1}{2(1+\nu)} \\
&J_{11} = \frac{E_2}{1-\nu^2} + \frac{E_{2s} d_s}{S_s}; \quad J_{22} = \frac{E_2}{1-\nu^2} + \frac{E_{2r} d_r}{S_r} \\
&J_{12} = \frac{E_2 \nu}{1-\nu^2}; \quad J_{33} = \frac{E_2}{2(1+\nu)} \\
&K_{11} = \frac{E_3}{1-\nu^2} + \frac{E_{3S} d_s}{S_s}; \quad K_{22} = \frac{E_3}{1-\nu^2} + \frac{E_{3r} d_r}{S_r} \\
&K_{12} = \frac{E_3 \nu}{1-\nu^2}; \quad K_{33} = \frac{E_3}{2(1+\nu)} \\
&T_1 = C_{11} e_{31} + C_{12} e_{32}; \quad T_2 = C_{12} e_{31} + C_{11} e_{32} \\
&F_1 = \left(\frac{h+h_p}{h_p}\right)[C_{11} e_{31} + C_{12} e_{32}] \\
&F_2 = \left(\frac{h+h_p}{h_p}\right)[C_{12} e_{31} + C_{11} e_{32}]
\end{aligned} \tag{A1}$$

where

$$\begin{aligned}
E_1 &= \int_{-h/2}^{h/2} E_{sh}(z,T) dz \\
&= \left(E_m(z,T) + \frac{E_c(z,T) - E_m(z,T)}{k+1}\right) h \\
E_2 &= \int_{-h/2}^{h/2} z E_{sh}(z,T) dz \\
&= \frac{\big(E_c(z,T) - E_m(z,T)\big) k h^2}{2(k+1)(k+2)} \\
E_3 &= \int_{-h/2}^{h/2} z^2 E_{sh}(z,T) dz \\
&= \Bigg[\frac{E_m(z,T)}{12} + \big(E_c(z,T) - E_m(z,T)\big) \\
&\quad \left(\frac{1}{k+3} + \frac{1}{k+2} + \frac{1}{4k+4}\right)\Bigg] h^3
\end{aligned} \tag{A2}$$

$$\begin{aligned}
E_{1i} &= \int_{-\left(\frac{h}{2}+h_s^T\right)}^{-\frac{h}{2}} E_s(z,T) dz \\
&= \int_{\frac{h}{2}}^{\frac{h}{2}+h_s^T} E_s(z,T) dz \\
&= \left(E_c(z,T) + \frac{E_m(z,T) - E_c(z,T)}{k_2+1}\right) h_s^T \\
E_{2i} &= \int_{-\left(\frac{h}{2}+h_s\right)}^{-\frac{h}{2}} z E_s(z,T) dz \\
&= \int_{\frac{h}{2}}^{\frac{h}{2}+h_s} z E_s(z,T) dz \\
&= \frac{E_c(z,T)}{2}\, h h_s^T \left(\frac{h_s^T}{h} + 1\right) \\
&\quad + \big(E_m(z,T) - E_c(z,T)\big)\, h h_s^T \\
&\quad \left(\frac{1}{k_2+2}\frac{h_s^T}{h} + \frac{1}{2k_2+2}\right) \quad ;\ i = s,\ r \\
E_{3i} &= \int_{-\left(\frac{h}{2}+h_s^T\right)}^{-\frac{h}{2}} z^2 E_s(z,T) dz \\
&= \int_{\frac{h}{2}}^{\frac{h}{2}+h_s^T} z^2 E_s(z,T) dz \\
&= \frac{E_c(z,T)}{3} {h_s^T}^3 \left(\frac{3}{4}\frac{h^2}{{h_s^T}^2} + \frac{3}{2}\frac{h}{h_s^T} + 1\right) \\
&\quad + \big(E_m(z,T) - E_c(z,T)\big) {h_s^T}^3 \\
&\quad \left[\frac{1}{k_2+3} + \frac{1}{k_2+2}\frac{h}{h_s^T} + \frac{1}{4(k_2+1)}\frac{h^2}{{h_s^T}^2}\right]
\end{aligned} \tag{A3}$$

Appendix B

$$
\begin{aligned}
&\Delta = I_{11}I_{22} - I_{12}^2; \quad I_{11}^* = \frac{I_{11}}{\Delta} \\
&I_{22}^* = \frac{I_{22}}{\Delta}; \qquad I_{12}^* = \frac{I_{12}}{\Delta}; \qquad I_{33}^* = \frac{1}{I_{33}} \\
&J_{11}^* = I_{22}^*J_{11} - I_{12}^*J_{12}; \quad J_{22}^* = I_{11}^*J_{22} - I_{12}^*J_{12} \\
&J_{12}^* = I_{22}^*J_{11} - I_{12}^*J_{12}; \quad J_{21}^* = I_{11}^*J_{22} - I_{12}^*J_{12} \\
&J_{33}^* = \frac{J_{33}}{I_{33}}; \\
&T_1^* = I_{22}^*T_1 - I_{12}^*T_2; \qquad T_2^* = I_{11}^*T_2 - I_{12}^*T_1
\end{aligned} \tag{B1}
$$

$$
\begin{aligned}
&K_{11}^* = K_{11} - J_{11}^*J_{11} - J_{21}^*J_{12}; \\
&K_{12}^* = K_{12} - J_{12}^*J_{11} - J_{22}^*J_{12} \\
&K_{21}^* = K_{12} - J_{21}^*J_{22} - J_{11}^*J_{12}; \\
&K_{22}^* = K_{22} - J_{22}^*J_{22} - J_{21}^*J_{12} \\
&K_{36}^* = K_{33} - J_{33}J_{33}^* \\
&F_1^* = J_{11}T_1^* + J_{12}T_2^* - F_1; \\
&F_2^* = J_{12}T_1^* + J_{22}T_2^* - F_2
\end{aligned} \tag{B2}
$$

$$
\begin{aligned}
&A = I_{11}^*m^4\pi^4 + (I_{33}^* - 2I_{12}^*)m^2n^2\pi^2\lambda^2 + I_{22}^*n^4\lambda^4 \\
&B = J_{21}^*m^4\pi^4 + (I_{11}^* + I_{22}^* - 2J_{33}^*)m^2n^2\pi^2\lambda^2 \\
&\quad +J_{12}^*n^4\lambda^4 - \frac{L^2}{R}m^2n^2; \\
&\lambda = \frac{L}{R}
\end{aligned} \tag{B3}
$$

$$
\begin{aligned}
&a_1 = \frac{1}{L^4\rho_1}\left(D + \frac{B^2}{A}\right), \quad a_2 = \frac{G}{L^4\rho_1}, \quad a_3 = \frac{L^2m^2\pi^2h}{L^4\rho_1} \\
&a_4 = \frac{L^2n^2\lambda^2h}{L^4\rho_1}, \qquad a_5 = \frac{2F_2^*}{R^2\pi^2\rho_1}
\end{aligned} \tag{B4}
$$

where

$$
\begin{aligned}
&D = K_{11}^*m^4\pi^4 + (K_{12}^* + K_{21}^* + 4K_{33}^*)m^2n^2\pi^2\lambda^2 \\
&\quad +K_{22}^*n^4\lambda^4 \\
&G = \left(\frac{n^4\lambda^4}{16I_{11}^*} + \frac{m^4\pi^4}{16I_{22}^*}\right)
\end{aligned} \tag{B5}
$$